

Article

# Non-Destructive X-ray Spectrometric and Chromatographic Analysis of Metal Containers and Their Contents, from Ancient Macedonia

Christos S. Katsifas <sup>1,2,\*</sup> , Despina Ignatiadou <sup>3</sup>, Anastasia Zacharopoulou <sup>1</sup>, Nikolaos Kantiranis <sup>4</sup> , Ioannis Karapanagiotis <sup>5</sup>  and George A. Zachariadis <sup>2</sup>

<sup>1</sup> Laboratory of Physico-Chemical Studies & Archaeometry, Archaeological Museum of Thessaloniki, 54013 Thessaloniki, Greece; anastasiazach@hotmail.com

<sup>2</sup> Laboratory of Analytical Chemistry, Department of Chemistry, Aristotle University, 54124 Thessaloniki, Greece; zacharia@chem.auth.gr

<sup>3</sup> Department of Sculpture, National Archaeological Museum, 10682 Athens, Greece; dignatiadou@culture.gr

<sup>4</sup> Department of Mineralogy, Petrology and Economic Geology, School of Geology, Aristotle University, 54124 Thessaloniki, Greece; kantira@geo.auth.gr

<sup>5</sup> Department of Management and Conservation of Ecclesiastical Cultural Heritage Objects, University Ecclesiastical Academy of Thessaloniki, N. Plastira 65, 54250 Thessaloniki, Greece; y.karapanagiotis@aeath.gr

\* Correspondence: chkatsifas@culture.gr, Tel.: +30-6944-262-282

Received: 1 April 2018; Accepted: 31 May 2018; Published: 11 June 2018



**Abstract:** This work describes a holistic archaeometric approach to ancient Macedonian specimens. In the region of the ancient city Lete, the deceased members of a rich and important family were interred in a cluster of seven tombs (4th century BC). Among the numerous grave goods, there was also a set of metal containers preserving their original content. The physico-chemical analysis of the containers and their contents was performed in order to understand the purpose of their use. For the containers, Energy Dispersive micro-X-Ray Fluorescence (ED $\mu$ XRF) spectroscopy was implemented taking advantage of its non-invasive character. The case (B35) and the small pyxis (B37) were made of a binary Cu-Sn alloy accompanied by a slight amount of impurities (Fe, Pb, As) and the two miniature bowls were made of almost pure Cu. For the study of the contents, a combination of ED $\mu$ XRF, X-Ray Diffraction (XRD), and Gas Chromatography—Mass Spectrometry (GC-MS) was carried out. Especially for the extraction of the volatile compounds, the Solid Phase Micro-Extraction (SPME) technique was used in the headspace mode. Because of the detection of Br, High Pressure Liquid Chromatography coupled to a Diode-Array-Detector (HPLC-DAD) was implemented, confirming the existence of the ancient dye shellfish purple (porphyra in Greek). The analytical results of the combined implementation of spectrometric and chromatographic analytical techniques of the metal containers and their contents expand our knowledge about the pharmaceutical practices in Macedonia during the 4th century BC.

**Keywords:** Derveni; Ancient Macedonia; micro-XRF; XRD; HPLC-DAD; HS-SPME/GC-MS; ancient medicines; ancient pharmaceuticals; shellfish purple; porphyra; high-tin bronzes; bronzes

## 1. Introduction

The Derveni tombs were accidentally revealed in 1962, 9.5 km NW of Thessaloniki, Macedonia, Greece. The six cist graves and one Macedonian tomb that were excavated then had not been looted and contained rich offerings, mainly dated to the 4th century BC. The deceased were members of a rich and important Thessalian family that probably lived in the nearby ancient city Lete. In grave A, the so-called Derveni papyrus was found; fragments of a papyrus roll with the most important Orphic

religious text of the 4th century BC, preserving excerpts of an earlier poem. The biggest and richest grave was grave B. It contained the cremated remains of a man and his female consort, which had been placed in an elaborate bronze vessel, today known as the famous Derveni krater. That male individual was an important member of the elite, probably a royal companion who died when he was approximately 35–50 years old. In addition to the bronze krater, the burial contained a gold wreath and other gold jewelry, twenty silver vessels, many bronze vessels, stone alabastra, glass vessels and pottery vases, the iron weapons of the dead, a folding board gaming set with glass gaming counters, pieces of a leather cuirass, bronze greaves, and a gold coin of King Philip II [1,2].

Among the numerous grave goods, from grave B, was a lidded box (B35), preserving its original content (Figure 1). It is a semi-cylindrical case divided into three compartments. Each compartment is filled with a mass of “clay”. The case has a hinged lid that protects the contents. According to the first estimations [1], B35 is a case for storing cosmetics and its contents are materials for makeup. Ongoing research on the history of medicine in Macedonia and the comparison with other metal cases which have been unearthed in Macedonian burials [3,4], after B35, had led to suspicions that the Derveni case was a medical case. Other metal finds from the same grave that were more or less associated with the case B35 are: two bowls (B43a, B43b) and a pyxis (B37), all preserving their original content. In the two bowls, there are preserved pieces of a thin dark-coloured cake and in the pyxis there is a red powder.



**Figure 1.** Metal containers and their contents. (a) Lidded case B35 and its content (cakes B35-I, B35-II, B35-III). (b) Case B35 without the lid. (c) Bowls B43a and B43b. (d) Lidded pyxis B37 (with and without lid).

The aims of the present physico-chemical study are: (a) to determine the composition of the alloy used for the construction of the metal containers, as well as the differentiation according to each part of the artefact (e.g., body, lid, handle, nails); and (b) to identify the inorganic and organic components of the contents using chemical and mineralogical analysis. The analytical results will contribute to the effort to determine the nature of these artefacts and consequently their purpose of use, as well as to illuminate the identity of their owner.

## 2. Materials and Methods

The metal containers under study are: one lidded case (B35), two miniature bowls (B43a, B43b), and a small pyxis (B37), all found in Derveni grave B. The metal case B35 consists of different parts: body, lid, handle, the lid's hinges, the rim of the case proper, and the nails the latter is fastened with. The bowls B43a and B43b have been made from a single metal sheet and pyxis B37 consists of its body and a lid. Case B35 is preserved in very good condition. It has been chemically cleaned in the past and does not carry any corrosion products. Its color, after the cleaning, is golden. On the other hand the two bowls (B43a, B43b) are reddish, denoting a differentiation of the alloy compared to that of B35. They are also preserved in a very good state and apparently do not present corrosion layers. Finally, pyxis B37 presents, at the body, a thick reddish corrosion layer in combination with extensive restoration works. Its lid maintains a better condition with areas where the metal does not present extensive corrosion layers.

For the analysis of the metal containers, the choice of a non-invasive and non-destructive analytical technique is obligatory. Sampling is largely prohibited, according to the Greek Archaeological Law, due to the uniqueness, integrity, and small size of the artefacts. So the choice of a non-invasive technique like Energy Dispersive micro X-ray Fluorescence (ED $\mu$ XRF) spectroscopy—which is a widespread technique for the analysis of ancient metals [5,6]—was a requisite instead of a technique that provides bulk analysis, such as Inductively Coupled Plasma Spectroscopy (ICP) or Atomic Absorption Spectroscopy (AAS). On the other hand, ED $\mu$ XRF provides a chemical profile of the surface, which may differ from the bulk composition and perhaps is not representative of the whole [7,8]. When bronze artefacts are exposed to the atmosphere or are buried in the ground, their surface acquires a more or less thick patina under which the metal core may remain substantially unchanged [9]. Before the implementation of the ED $\mu$ XRF analysis, optical macro- and microscopic examination of each artefact was applied in order to select the spots for analysis. Areas free of corrosion products or materials from conservation treatments were selected. Especially at the pyxis B37, mechanical removal of the corrosion products took place in order to measure from the bulk of the metal.

The contents of case B35 bear similar hues. Starting from left to right, they were numbered: B35-I, B35-II, and B35-III. Especially at the middle compartment of B35 and on the top of cake B35-II, a fourth cake can be seen which has a different hue than the others. Instead of an earthy hue, it is reddish and was hence numbered B35-IIa. Macroscopically, cakes B35-I, B35-II, and B35-III resemble dried out clays. Respectively, the contents of bowls B43a and B43b were numbered B43a-I and B43b-I. These cakes are harder than those in case B35 and their hue is brownish red with a dark top. To characterize the components of the four cakes that are preserved in the lidded case B35, as well as the two from the bronze bowls (B43a, B43b) and the red powder from the pyxis (B37), a physico-chemical analysis was undertaken in combination with a mineralogical examination. After the preliminary morphological examination by stereomicroscopy, ED $\mu$ XRF spectroscopy was carried out for the analysis of the inorganic constituents. In order to determine their mineralogical composition, XRD diffractometry was implemented. For the study of the organic constituents, the samples were extracted with the Head Space—Solid Phase Micro-Extraction (HS-SPME) technique and the absorbed volatiles were analyzed by Gas Chromatography—Mass Spectrometry (GC-MS). Because of the significance of the material under study, an effort has been made to implement the above analytical techniques, as much as possible, in a non-destructive way. Analysis using High Pressure Liquid Chromatography coupled to a Diode-Array-Detector (HPLC-DAD) was carried out in only one sample from cake B35-IIa in order to ascertain the constituent which is responsible for its color. The cause of this implementation was the interesting results of ED $\mu$ XRF in combination with its reddish hue.

### 2.1. Energy Dispersive Micro-X-ray Fluorescence spectrometry (ED $\mu$ XRF)

The instrument ARTAX 400 (Bruker AXS Microanalysis GmbH, Berlin, Germany) was used for the implementation of the micro-X-ray Fluorescence spectroscopy technique ( $\mu$ XRF). This Energy Dispersive spectrometer has been specially designed for the demands of archaeometry [10].

The measuring head, which is placed on a  $x,y,z$ —motor driven positioning stage, is comprised of: (a) an air cooled Mo X-ray fine focus tube, (b) a peltier cooled silicon drift detector (SDD), and (c) a Charge Coupled Device (CCD) camera for the visual inspection of the sample. The X-ray beam is restricted by a collimator and on the surface of the sample has a diameter between 200  $\mu\text{m}$  and 1500  $\mu\text{m}$ , depending on the type of collimator used. All excitation and detection paths can be rinsed with Helium (He) gas which is directed, by use of two gas jets, towards the sample surface in order to reduce the absorption of the beam through the air and thus improve the excitation conditions for elements with a lower atomic number. Acquired spectra were processed with software SPECTRA 7.4. This program enables the acquisition of measurement data including the control of all Artax 400 components. Parallel to the measurement, it is possible to carry out qualitative elemental analysis, data reduction (integral calculation of the different spectral lines through deconvolution), and calculation of the artefact elemental concentration.

For the analysis of the metal containers, ED $\mu$ XRF measurements (ARTAX 400, Bruker AXS Microanalysis GmbH, Berlin, Germany) were taken in order to determine their elemental composition. For the metal case B35, measurements were taken from every different part (body, lid, hinge, rim, nails). Each final reported result is the mean value of three measurements. The measurement time for each spot analysis was 100s. The voltage of the exciting X-ray beam was 50 kV and the current was 700  $\mu\text{A}$ . The collimator with a 1500  $\mu\text{m}$  diameter was used in order to get a representative result and to avoid alterations due to micro structural inhomogeneity [11,12]. Especially for the analysis of the pyxis B37, which presents corrosion layers, and in order to avoid the removal of corrosion in an extended area (since it is considered as a destructive action), the collimator with a diameter of 650  $\mu\text{m}$  was used. The certified data from Certified Reference Material (CRM) 32XSN1 (MBH—Analytical Ltd., Barnet, UK) was used as a calibration file. The quantified results were balanced to 100%. In order to check the accuracy of the implemented method, measurements were taken with the same parameters as those employed for the artefacts, from Certified Reference Materials (CRMs). BCR-691 (European Commission—Joint Research Centre, Institute for Reference Materials and Measurements, Brussels, Belgium), a set of five (5) copper alloys, was used (Table 1).

**Table 1.** Results of the analysis of Certified Reference Materials (CRM's) and detection limits (wt %).

	BCR-691	Sn	Zn	Pb	As
Quaternary bronze (A)	Certified value $\pm$ uncertainty	7.16 $\pm$ 0.21	6.02 $\pm$ 0.22	7.90 $\pm$ 0.7	0.19 $\pm$ 0.01
	Measured value $\pm$ std	7.00 $\pm$ 0.3	6.20 $\pm$ 0.45	7.50 $\pm$ 0.50	0.20 $\pm$ 0.00
Brass (B)	Certified value $\pm$ uncertainty	2.06 $\pm$ 0.07	14.80 $\pm$ 0.50	0.39 $\pm$ 0.04	0.10 $\pm$ 0.01
	Measured value $\pm$ std	2.00 $\pm$ 0.10	14.50 $\pm$ 0.21	0.30 $\pm$ 0.06	0.10 $\pm$ 0.00
Arsenic copper (C)	Certified value $\pm$ uncertainty	0.202 $\pm$ 0.029	0.05 $\pm$ 0.005	0.175 $\pm$ 0.014	4.6 $\pm$ 0.27
	Measured value $\pm$ std	0.17 $\pm$ 0.06	0.03 $\pm$ 0.01	0.18 $\pm$ 0.04	4.5 $\pm$ 0.50
Lead bronze (D)	Certified value $\pm$ uncertainty	10.1 $\pm$ 0.80	0.148 $\pm$ 0.024	9.2 $\pm$ 1.7	0.285 $\pm$ 0.022
	Measured value $\pm$ std	9.60 $\pm$ 0.50	0.17 $\pm$ 0.02	9.05 $\pm$ 0.416	0.26 $\pm$ 0.05
Tin bronze (E)	Certified value $\pm$ uncertainty	7 $\pm$ 0.60	0.157 $\pm$ 0.025	0.204 $\pm$ 0.018	0.194 $\pm$ 0.02
	Measured value $\pm$ std	7.33 $\pm$ 0.50	0.17 $\pm$ 0.01	0.2 $\pm$ 0.00	0.2 $\pm$ 0.00
Estimated detection limits (%)		0.02	0.01	0.03	0.01

For the elemental analysis of the contents of the metal containers, with the ED $\mu$ XRF technique, the voltage of the exciting X-ray beam was 35 kV and the current was 900  $\mu\text{A}$ . It was also implemented in an He gas atmosphere. The 1500  $\mu\text{m}$  diameter collimator was used to counterbalance the inhomogeneity of the materials under study. Each final reported result is the mean value of seven measurements since the contents present greater inhomogeneity than the metal containers. For the quantification of the analytical results, the CRM soil sample SO-3 (Canada Centre for Mineral & Energy Technology, Ottawa, ON, Canada) was used in combination with software SPECTRA 7.4 (Bruker AXS Microanalysis GmbH, Berlin, Germany).

## 2.2. X-ray Diffraction (XRD)

The content of the metal containers were archaeological material and therefore were studied in their bulk form without any grinding, homogenization, or pretreatment. In order to identify their mineralogical composition, X-ray diffraction analysis (XRD) was applied directly on the surface of the samples.

A Phillips PW1820/00 diffractometer equipped with a PW1710/00 microprocessor (PHILIPS, Almelo, The Netherlands) was used and the samples were scanned over the  $3^{\circ}$ – $63^{\circ}$   $2\theta$  interval at a scanning speed of  $1.2^{\circ}/\text{min}$ . Semi-quantitative analysis estimates of the abundance of the mineral phases were derived from the XRD data, using the intensity of a certain reflection [13], the density, and the mass absorption coefficient for Cu- $K_{\alpha}$  radiation for the minerals present. The identification of the minerals present was made using the DDView<sup>+</sup>/SiIeve<sup>+</sup> ICDD's viewing/search indexing software provided with the PDF-4<sup>+</sup> (PDF-4<sup>+</sup>, 2009, Powder diffraction file<sup>TM</sup>, International Centre for Diffraction Data, Newtown Square, PA, USA) relational database. Corrections were made using the external standard mixtures of minerals (i.e., standard mixtures of the identified minerals in the studied samples such as quartz and cristobalite, feldspars, micas and chlorite, amphibole, calcite and sulfate minerals, as well as iron oxides). The detection limit of the method was  $\pm 1\%$   $w/w$  [14]. The degree of crystallinity and the calculation of the amorphous phase amount were calculated according to the method described by Kantiranis et al. (2004) [14].

## 2.3. Head Space—Solid Phase Micro-Extraction/Gas Chromatography—Mass Spectrometry (HS—SPME/GC—MS)

The pre-treatment and extraction of the samples was done by the HS-SPME technique using a polydimethylsiloxane (PDMS) coated fiber (100  $\mu\text{m}$  film) in the head space above the heated samples. GC-MS (Agilent 6873 K gas chromatograph—Agilent 5973 quadrupole mass detector, Agilent Technologies, Santa Clara, CA, USA) analysis of the absorbed volatiles from the samples was carried out and finally the identification of the compounds was succeeded by using the NIST library. The GC-MS operating conditions are listed in Table 2.

**Table 2.** GC-MS operating conditions.

Operating Conditions	Value
GC model	Agilent 6873 K gas chromatograph (Electron Ionization mode)
Column DB-5MS (capillary)	30 m $\times$ 0.25 mm $\times$ 0.10 $\mu\text{m}$
Injector port temperature	200 $^{\circ}\text{C}$ (SPME fiber was remained there for 6 min)
Carrier gas, Flow-rate	Helium, 2.0 mL/min (constant pressure at 29.8 psi)
Oven temperature program	60 $^{\circ}\text{C}$ (3 min) to 270 $^{\circ}\text{C}$ , 10 $^{\circ}\text{C}/\text{min}$ ramp time
Transfer line temperature	250 $^{\circ}\text{C}$
MS model	Agilent 5973 quadrupole mass detector (Scan mode)
Total time of chromatographic analysis	40 min

## 2.4. High Pressure Liquid Chromatography—Diode Array Detector (HPLC-DAD)

High Pressure Liquid Chromatography was coupled to a Diode-Array-Detector (Ultimate 3000, Dionex, Sunnyvale, CA, USA,) and consisted of a LPG-3000 quaternary HPLC pump with a vacuum degasser, a WPS-3000SL auto sampler, a column compartment TCC-3000SD, and a UV-Vis Diode Array Detector (DAD-3000) (Dionex, Sunnyvale, CA, USA) Analyses were carried out by injecting 20  $\mu\text{L}$  into an Alltima (Grace-Alltech, Deerfield, IL, USA) HP C18 (250 mm  $\times$  3 mm, i.d. 5  $\mu\text{m}$ ) column at a stable temperature of 35  $^{\circ}\text{C}$ .

Two solvent reservoirs, containing (A) water + 0.1% ( $v/v$ ) Tri-Fluoro-Acetic Acid (TFA) and (B) acetonitrile + 0.1% ( $v/v$ ) TFA, were used under a gradient elution program which was developed and evaluated for the analysis of shellfish purple components offering extremely low limits of detection [15].

The sample was immersed in a hot (80  $^{\circ}\text{C}$ ) dimethyl sulfoxide (DMSO) bath and kept there for 15 min. After centrifugation, the upper liquid phase was immediately submitted to HPLC.

By employing this method, polar and apolar compounds are detected. The method was previously devised and optimised for the extraction and solubilisation of shellfish purple, as described in detail elsewhere [16].

### 3. Results

#### 3.1. Metal Containers

According to the results of Table 3, the main parts (body, lid, and rim) of the metal case B35 were made of copper-tin (Cu-Sn) alloy. Lead (Pb), iron (Fe), and calcium (Ca) were detected, at all parts, at quantities much lower than 1 wt %. Arsenic (As) is also detected, except at the four nails which present significant differentiation, at their chemical composition, compared to the main parts of B35. They consist of almost pure Cu which is detected at levels higher than 99.0 wt %. Nickel (Ni) and titanium (Ti) are only detected at the nails of B35, at very low quantities (rounded average for the four nails are:  $0.17 \pm 0.03$  and  $0.01 \pm 0.00$  wt % for Ni and Ti, respectively), while Sn is present at levels below 1 wt %. Another part of B35 that presents a significant differentiation is the hinge of the lid where the quantity of Sn ( $6.56 \pm 0.30$  wt %) is very low compared to the body of the case ( $12.11 \pm 0.20$  wt %).

Bowls B43a and B43b present the same qualitative and quantitative analysis. Cu is detected at levels around 99 wt %. The two bowls present also the same chemical elements Sn, Pb, Fe, As, Ni, and Ca at similar quantities (lower than 0.5 wt %). At pyxis B37, measurements were only taken from its lid after the removal of superficial corrosion products. The body presents thick corrosion layers which will not provide us with a safe quantitative result. The lid of pyxis B37 mainly consists of Cu ( $86.96 \pm 0.40$  wt %) and Sn ( $12.16 \pm 0.20$  wt %) at quantities similar to the main parts of the metal case B35, e.g., the body (Cu:  $87.61 \pm 0.60$  wt % and Sn:  $12.16 \pm 0.20$  wt %). Similar to B35, Pb and Fe are the minor elements, at quantities lower than 1 wt %. However, Ni is only detected at a very low quantity ( $0.15 \pm 0.50$  wt %).

#### 3.2. Contents of the Metal Containers

According to the ED $\mu$ XRF analysis (Table 4), cakes B35-I, B35-II, and B35-III, which present a similar appearance, texture, and colour, also present similar analytical results. Major constituents (concentration higher than 1 wt %) are: SiO<sub>2</sub>, Al<sub>2</sub>O<sub>3</sub>, Fe<sub>2</sub>O<sub>3(total)</sub>, MgO, CaO, CuO, and K<sub>2</sub>O; and minor constituents (concentration between 0.1 wt % and 1.0 wt %) are: V<sub>2</sub>O<sub>3</sub>, and MnO. Finally, at the level of traces (concentration lower than 0.1 wt %), the following were detected: Cr<sub>2</sub>O<sub>3</sub>, NiO, ZnO, Rb<sub>2</sub>O, SrO, and PbO.

Cake B35-IIa, which presents a reddish hue, presents some differentiations compared to the other cakes. Al<sub>2</sub>O<sub>3</sub>, which is a main constituent in the other cakes, is a minor one at B35-IIa ( $0.28 \pm 0.30$  wt %). Furthermore, the total percentage of the inorganic constituents is lower in than the other cakes and ranges from 16.56 wt % to 42.27 wt %. Finally, B35-IIa is the only cake where the chemical element bromine (Br) was detected (Figure 2). This result, in combination with the differentiation of the colour of the cake (reddish hue), created suspicions for the possible existence of a dye. In the cakes (B43a-I, B43b-I) of the two bowls, there is a similar distribution between major and minor constituents and those that detected as traces. Compared to cakes of the metal case B35, the total percentage of the inorganic oxides ( $30.98$  wt % for cake B43a-I and  $15.03$  wt % for cake B43b-I) is significantly lower. The powder in pyxis B37 presents great differentiations, in terms of the analytical results, compared to the contents of the others containers. There are only two major constituents: Fe<sub>2</sub>O<sub>3(t)</sub> ( $11.44 \pm 1.10$  wt %) and CuO ( $9.71 \pm 1.10$  wt %). The minor constituent detected is CaO, and ZnO and K<sub>2</sub>O are only detected in traces.

**Table 3.** Chemical composition (wt % ± std) of metal containers—results of EDμXRF analysis (\* nd: not detected).

No	Description	Cu	Sn	Pb	Fe	As	Ni	Ca	Ti
1	B35-body	87.61 ± 0.60	12.11 ± 0.20	0.19 ± 0.04	0.06 ± 0.02	0.02 ± 0.01	nd*	0.01 ± 0.00	nd
2	B35-lid	87.68 ± 0.50	12.07 ± 0.30	0.12 ± 0.02	0.08 ± 0.03	0.04 ± 0.01	nd	0.02 ± 0.01	nd
3	B35-lid-handle	85.33 ± 0.30	14.42 ± 0.20	0.15 ± 0.03	0.06 ± 0.02	0.01 ± 0.00	nd	0.03 ± 0.01	nd
4	B35-lid-hinge	93.00 ± 0.60	6.59 ± 0.30	0.23 ± 0.04	0.13 ± 0.05	0.03 ± 0.01	nd	0.02 ± 0.01	nd
5	B35 body-rim	83.44 ± 0.30	15.62 ± 0.50	0.72 ± 0.04	0.04 ± 0.02	0.01 ± 0.00	nd	0.02 ± 0.01	nd
6	B35-nail-01	99.20 ± 0.60	0.06 ± 0.01	0.35 ± 0.03	0.20 ± 0.03	nd	0.17 ± 0.03	0.01 ± 0.00	0.01 ± 0.00
7	B35-nail-02	98.95 ± 0.50	0.76 ± 0.20	0.40 ± 0.02	0.18 ± 0.04	nd	0.17 ± 0.03	0.02 ± 0.00	0.01 ± 0.00
8	B35-nail-03	99.22 ± 0.50	0.10 ± 0.02	0.34 ± 0.04	0.15 ± 0.02	nd	0.16 ± 0.03	0.02 ± 0.01	nd
9	B35-nail-04	99.09 ± 0.60	0.12 ± 0.40	0.43 ± 0.06	0.17 ± 0.08	nd	0.16 ± 0.03	0.01 ± 0.00	0.01 ± 0.00
10	B43a-body	99.20 ± 0.40	0.04 ± 0.01	0.45 ± 0.05	0.14 ± 0.05	0.01 ± 0.00	0.16 ± 0.03	0.01 ± 0.00	nd
11	B43b-body	99.12 ± 0.50	0.04 ± 0.01	0.48 ± 0.02	0.18 ± 0.03	0.01 ± 0.00	0.17 ± 0.03	0.01 ± 0.00	nd
12	B37-lid	86.96 ± 0.40	12.16 ± 0.20	0.66 ± 0.04	0.07 ± 0.02	nd	0.15 ± 0.05	nd	nd

**Table 4.** Contents of metal containers—results of the EDμXRF analysis (wt %).

Description	SiO <sub>2</sub>	TiO <sub>2</sub>	Al <sub>2</sub> O <sub>3</sub>	Fe <sub>2</sub> O <sub>3(t)</sub>	V <sub>2</sub> O <sub>3</sub>	Cr <sub>2</sub> O <sub>3</sub>	MnO	MgO	CaO	CuO	NiO	ZnO	Rb <sub>2</sub> O	SrO	PbO	K <sub>2</sub> O	Br	TOTAL
<b>B35-I</b>	42.66 ± 2.10	1.42 ± 0.30	15.53 ± 1.20	10.38 ± 1.10	0.18 ± 0.06	0.09 ± 0.04	0.31 ± 0.10	2.19 ± 0.20	4.90 ± 0.42	2.30 ± 0.32	0.01 ± 0.00	0.01 ± 0.00	0.02 ± 0.01	0.04 ± 0.02	0.01 ± 0.00	3.36 ± 0.45	nd	<b>83.41</b>
<b>B35-II</b>	29.84 ± 1.40	0.82 ± 0.20	10.75 ± 0.40	5.95 ± 0.40	0.10 ± 0.04	0.04 ± 0.02	0.18 ± 0.02	0.86 ± 0.40	3.12 ± 0.25	4.12 ± 0.70	nd	0.01 ± 0.00	0.01 ± 0.00	0.02 ± 0.01	0.02 ± 0.01	1.84 ± 0.28	nd	<b>57.70</b>
<b>B35-IIa</b>	16.58 ± 1.20	0.43 ± 0.12	0.28 ± 0.30	4.65 ± 1.00	0.04 ± 0.03	0.15 ± 0.05	0.06 ± 0.03	0.90 ± 0.20	4.67 ± 0.32	11.85 ± 1.56	0.03 ± 0.01	0.02 ± 0.01	0.02 ± 0.01	0.01 ± 0.00	0.01 ± 0.00	1.02 ± 0.04	0.40 ± 0.05	<b>41.14</b>
<b>B35-III</b>	43.94 ± 2.15	1.22 ± 0.30	18.06 ± 1.80	9.92 ± 1.10	0.22 ± 0.04	0.07 ± 0.03	0.10 ± 0.02	1.84 ± 0.35	2.00 ± 0.24	2.02 ± 0.35	0.01 ± 0.00	0.01 ± 0.00	0.02 ± 0.01	0.02 ± 0.01	0.14 ± 0.03	2.92 ± 0.67	nd	<b>82.53</b>
<b>B43a-I</b>	6.48 ± 1.20	0.35 ± 0.15	2.19 ± 0.25	3.57 ± 0.70	0.75 ± 0.25	0.12 ± 0.02	0.03 ± 0.01	0.86 ± 0.25	3.65 ± 0.18	12.02 ± 1.32	0.04 ± 0.02	0.01 ± 0.00	nd	0.01 ± 0.00	0.16 ± 0.00	0.73 ± 0.25	nd	<b>30.98</b>
<b>B43b-I</b>	4.43 ± 0.80	0.22 ± 0.30	1.10 ± 0.20	2.42 ± 0.40	0.44 ± 0.10	0.07 ± 0.03	0.01 ± 0.00	0.63 ± 0.18	1.78 ± 0.16	3.39 ± 0.88	0.03 ± 0.01	nd	nd	0.01 ± 0.00	0.10 ± 0.00	0.41 ± 0.25	nd	<b>15.03</b>
<b>B37-I</b>	nd	nd	nd	11.44 ± 1.10	nd	nd	nd	nd	0.27 ± 0.08	9.71 ± 1.10	nd	0.02 ± 0.00	nd	nd	nd	0.02 ± 0.00	nd	<b>21.47</b>

nd: not detected.

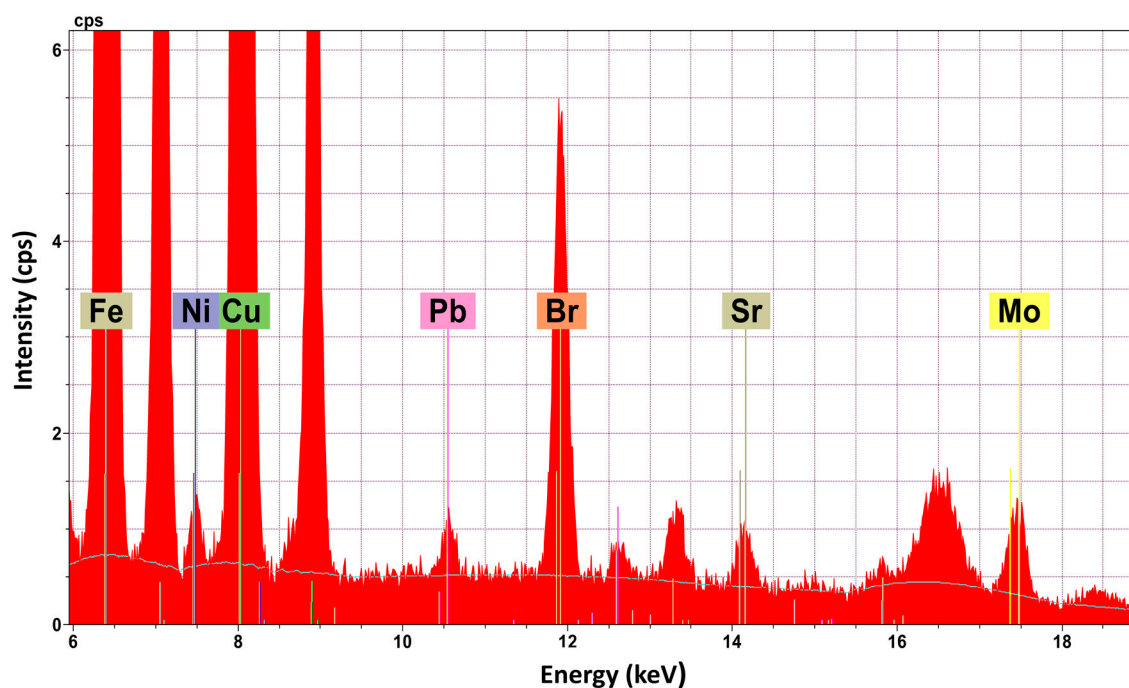


**Figure 2.** ED $\mu$ XRF spectrum of cake B-35-IIa—detection of Br (peak  $K_{\alpha 1}$  at 11.88 keV and  $K_{\beta 1}$  at 13.29 keV).

The detection of Br in combination with the colour differentiation of the sample B35-IIa led to the investigation of the possible existence of a dye that contains Br. The implementation of the HPLC-DAD technique resulted in the detection of the compound 6,6'-dibromoindigotin (DBI) (Figure 3), which was detected at 288 nm. The limit of daltons is  $2.4 \times 10^{14}$ , as described in detail elsewhere [13].

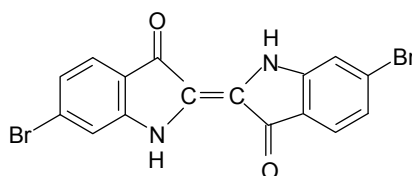


**Figure 3.** 6,6'-dibromoindigotin (DBI).

According to the results of the mineralogical analysis (Table 5) of the cakes in case B35, similar amounts of quartz ( $\text{SiO}_2$ ) (39–44 wt %) were detected at high quantities. Other constituents in abundance are: plagioclase (8–29 wt %), mica (6–14 wt %) that belongs to the group of silicate minerals, and chlorite (4–8 wt %). Minerals like K-feldspar and calcite are only detected in cakes B35-II and B35-III. Amorphous matter estimated at high level ranges from 16% to 31%, except in cake B35-I, where it is only 5 wt %. In cakes B43a-I and B43b-I, the amorphous matter estimated at even higher levels ranges from 65 wt % to 78 wt %. Except for the siliceous minerals (quartz, plagioclase, and mica), cristobalite (6–12 wt %), gypsum (5 wt %), and graphite (1 wt %) were also detected. Graphite was possible to identify (Figure 4) and measure using the 89-8487 ICDD card (main peak  $3.3540 \text{ \AA}$ , in comparison with the  $3.3434 \text{ \AA}$  main peak of quartz, 46-1045 ICDD card). Especially 2 wt % bassanite was detected in cake B43b-I, a calcium sulfate mineral. Finally, powder B37-I presented a very different mineralogical composition than the others. The dominant constituents are the ferrous oxides (hematite and magnetite: 71 wt %), a copper sulphate mineral antlerite (15 wt %), gypsum (8 wt %), bassanite (5 wt %), and a low quantity of a rare borate mineral: inderite (1 wt %).

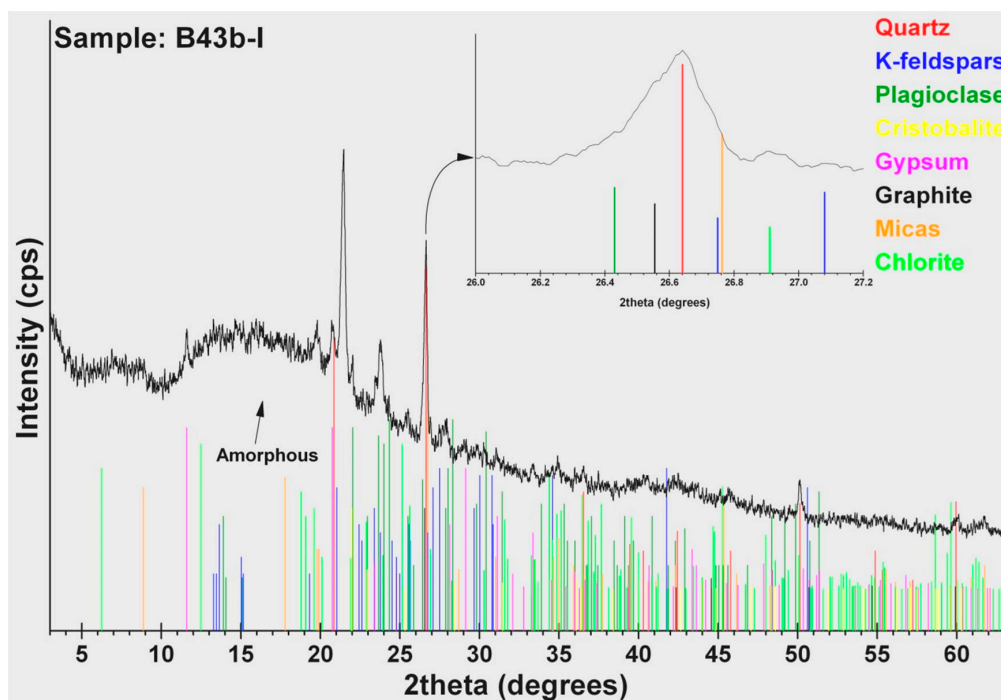


Figure 4. XRD pattern of cake B43b-I.

Table 5 presents the organic constituents of the contents of the metal containers according to the results of the HS-SPME/GC-MS analysis. In cake B35-I, only three (3) organic compounds were detected, none were detected at B35-II, and only three (3) (most of them fatty acids) were detected at B35-III. Contrary to the above, in cake B35-IIa, which presents a reddish hue, twenty-two (22) organic constituents (fatty acids, fatty acid esters, hydrocarbons, quinolines, phthalate esters, and amines) were detected (Figure 5). At contents B43a-I and B43b-I, the same three organic constituents were detected and at the red powder B37-I, seven (7) (thioamides, lactam, hydrocarbons, halide, and phthalate ester) were detected. Except for B43a-I and B43b-I, the other contents do not share any of the organic compounds. Fatty acids are the class of organic compounds which is common in the B35 and B43 contents. On the other hand, classes like thioamides and lactam are only detected at powder B37.

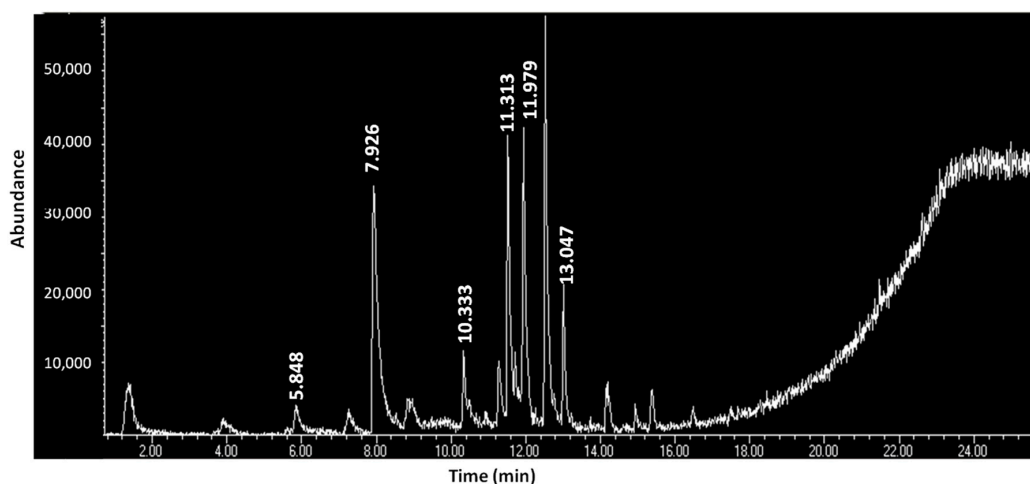


Figure 5. GC-MS chromatogram of volatile constituents of the sample B35-IIa (retention times correspond to analytes as described in Table 6).

**Table 5.** Contents of metal containers—results of the XRD analysis (wt %).

Sample	Quartz	Plagioclase	Mica	Chlorite	Dolomite	Amorphous	K-Feldspar	Calcite	Amphibole	Cristobalite	Gypsum	Graphite	Hydrozincite	Hematite	Magnetite	Bassanite	Inderite	Antlerite
B35-I	39	28	14	8	nd	5	nd	nd	5	nd	nd	nd	1	nd	nd	nd	nd	nd
B35-II	43	8	9	5	nd	18	7	7	3	nd	nd	nd	nd	nd	nd	nd	nd	nd
B35-IIa	42	9	8	7	3	31	nd	nd	nd	nd	nd	nd	nd	nd	nd	nd	nd	nd
B35-III	44	13	6	4	nd	16	8	6	3	nd	nd	nd	nd	nd	nd	nd	nd	nd
B43a-I	7	1	1	1	nd	78	nd	nd	nd	6	5	1	nd	nd	nd	nd	nd	nd
B43b-I	11	1	1	nd	nd	65	2	nd	nd	12	5	1	nd	nd	nd	2	nd	nd
B37-I	nd	nd	nd	nd	nd	nd	nd	nd	nd	nd	8	nd	nd	62	9	5	1	15

nd: not detected

**Table 6.** Contents of the metal containers: results of HS-SPME/GC-MS analysis.

No	RT (min)	Chemical Compound	Chemical Formula	B35-I	B35-II	B35-IIa	B35-III	B43a-I	B43b-I	B37-I
1	1.205	Ethanethioamide	C <sub>2</sub> H <sub>5</sub> NS	nd	nd	nd	nd	nd	nd	+
2	1.422	2,4-Hexadiyne	C <sub>6</sub> H <sub>6</sub>	nd	nd	+	nd	nd	nd	nd
3	1.827	2,4,6,8-tetramethyl-1-undecene	C <sub>15</sub> H <sub>30</sub>	nd	nd	nd	nd	nd	nd	+
4	1.841	Caprolactam	C <sub>6</sub> H <sub>11</sub> NO	nd	nd	nd	nd	nd	nd	+
5	2.587	Pentane, 2,3-dimethyl	C <sub>7</sub> H <sub>16</sub>	nd	nd	nd	nd	nd	nd	+
6	3.136	Napthalene-1-isocyano	C <sub>11</sub> H <sub>7</sub> N	nd	nd	nd	nd	nd	nd	+
7	3.151	1-Octanol, 2-butyl-	C <sub>12</sub> H <sub>26</sub> O	nd	nd	+	nd	nd	nd	nd
8	3.939	Propanoic acid, 2-methyl-,butylester	C <sub>8</sub> H <sub>16</sub> O <sub>2</sub>	nd	nd	+	nd	nd	nd	nd
9	5.848	Pentanoic acid	C <sub>19</sub> H <sub>30</sub> O <sub>3</sub>	nd	nd	+	nd	nd	nd	nd
10	7.267	Didodecyl phthalate	C <sub>32</sub> H <sub>54</sub> O <sub>4</sub>	nd	nd	+	nd	nd	nd	nd
11	7.926	1,3-Dioxolane-2-propanoic acid, 2-methyl-,ethylester	C <sub>9</sub> H <sub>16</sub> O <sub>4</sub>	nd	nd	+	nd	nd	nd	nd
12	8.855	Hexane, 3,3-dimethyl	C <sub>8</sub> H <sub>18</sub>	nd	nd	+	nd	nd	nd	nd
13	10.333	Nonadecane	C <sub>19</sub> H <sub>40</sub>	nd	nd	+	nd	nd	nd	nd
14	10.925	2,5,8,-Triphenylbenzotriazole	C <sub>24</sub> H <sub>15</sub> N <sub>9</sub>	nd	nd	+	nd	nd	nd	nd
15	10.932	8-Benzylquinoline	C <sub>16</sub> H <sub>13</sub> N	nd	nd	+	nd	nd	nd	nd
16	10.962	Benzimidazo[2,1-a]isoquinoline	C <sub>15</sub> H <sub>10</sub> N <sub>2</sub>	nd	nd	+	nd	nd	nd	nd
17	11.105	Butane, 1-chloro-3,3-dimethyl	C <sub>6</sub> H <sub>13</sub> Cl	nd	nd	nd	nd	+	+	+
18	11.249	1,2-Benzenedicarboxylic acid, bis[2-methylpropyl] ester	C <sub>16</sub> H <sub>22</sub> O <sub>4</sub>	nd	nd	+	nd	nd	nd	nd
19	11.284	Phthalic acid, 6-ethyl-3-octylisobutylester	C <sub>22</sub> H <sub>34</sub> O <sub>4</sub>	nd	nd	+	nd	nd	nd	nd
20	11.313	1,2-Benzenedicarboxylic acid, bis[2-methylpropyl] ester	C <sub>16</sub> H <sub>22</sub> O <sub>4</sub>	nd	nd	+	nd	nd	nd	nd

Table 6. Cont.

No	RT (min)	Chemical Compound	Chemical Formula	B35-I	B35-II	B35-IIa	B35-III	B43a-I	B43b-I	B37-I
21	11.569	6-Undecylamine	C <sub>11</sub> H <sub>25</sub> N	nd	nd	+	nd	nd	nd	nd
22	11.935	1,4-Oxathiin, 2,3-dihydro-6-methyl	C <sub>5</sub> H <sub>8</sub> O <sub>2</sub> S	nd	nd	+	nd	nd	nd	nd
23	11.979	Formic acid, ethoxymethylene hydrazide	C <sub>4</sub> H <sub>8</sub> N <sub>2</sub> O <sub>2</sub>	nd	nd	+	nd	nd	nd	nd
24	12.509	Dibutylphthalate	C <sub>16</sub> H <sub>22</sub> O <sub>4</sub>	nd	nd	nd	nd	+	+	+
25	12.515	Dibutylphthalate	C <sub>16</sub> H <sub>22</sub> O <sub>4</sub>	nd	nd	+	nd	nd	nd	nd
26	12.520	1,4-Benzenedicarboxylic acid, bis[2-methylpropyl] ester	C <sub>16</sub> H <sub>22</sub> O <sub>4</sub>	nd	nd	+	nd	nd	nd	nd
27	12.586	Dibutylphthalate	C <sub>16</sub> H <sub>22</sub> O <sub>4</sub>	nd	nd	+	nd	nd	nd	nd
28	13.007	Sulfurous acid, butyldecylester	C <sub>14</sub> H <sub>30</sub> O <sub>3</sub> S	nd	nd	nd	nd	+	+	nd
29	13.047	Nonadecane, 2-methyl-	C <sub>20</sub> H <sub>42</sub>	nd	nd	+	nd	nd	nd	nd
30	14.166	Morpholineethanamine	C <sub>6</sub> H <sub>14</sub> N <sub>2</sub> O	nd	nd	+	nd	nd	nd	nd
31	14.203	Thiophene3-(1,1-dimethylethoxy)	C <sub>8</sub> H <sub>12</sub> OS	nd	nd	+	nd	nd	nd	nd
32	14.956	<i>p</i> -Terphenyl	C <sub>18</sub> H <sub>14</sub>	nd	nd	+	nd	nd	nd	nd
33	15.417	2-Piperidinecarboxylic acid, methylester, PFP	C <sub>10</sub> H <sub>12</sub> F <sub>5</sub> NO <sub>3</sub>	nd	nd	+	nd	nd	nd	nd
34	16.485	1-(Prop-2-ynyl)-3,3-bis(trifluoromethyl)diaziridine	C <sub>6</sub> H <sub>4</sub> F <sub>6</sub> N <sub>2</sub>	nd	nd	+	nd	nd	nd	nd
35	24.458	Boron, bis{μ-[(3,5-bis(1,1-dimethylethyl)-1-H-pyrazolato-N1:N2)]diethyl-	C <sub>26</sub> H <sub>50</sub> B <sub>2</sub> N <sub>4</sub>	nd	nd	nd	+	nd	nd	nd
36	25.072	10-Ethyl-3-chloro-7-( <i>N-p</i> -nitrobenzylideneamino)-phenothiazine	C <sub>21</sub> H <sub>16</sub> ClN <sub>3</sub> O <sub>2</sub> S	nd	nd	nd	+	nd	nd	nd
37	27.215	Yohimban-16-carboxylic acid, 17-hydroxy-10-methoxy-, methylester	C <sub>22</sub> H <sub>28</sub> N <sub>2</sub> O <sub>4</sub>	+	nd	nd	nd	nd	nd	nd
38	28.978	Hexadecanoic acid, 2-hydroxy-1,3-propanediylester	C <sub>35</sub> H <sub>68</sub> O <sub>5</sub>	+	nd	nd	nd	nd	nd	nd
39	30.384	9-Octadecanoic acid ( <i>Z</i> )-2 hydroxy-1,3-propanediylester	C <sub>39</sub> H <sub>72</sub> O <sub>5</sub>	nd	nd	nd	+	nd	nd	nd
40	38.123	9-Octadecanoic acid ( <i>Z</i> )-2 hydroxy-3- propanediylester	C <sub>37</sub> H <sub>70</sub> O <sub>5</sub>	+	nd	nd	nd	nd	nd	nd

+: detected, nd: not detected.

## 4. Discussion

### 4.1. Metal Containers

Metal case B35, which was found in Derveni grave B, presents differentiation in terms of the chemical composition of its various parts (Table 2). These parts have been made from hammered metal sheets (except the lid's handle which was cast). In general when Sn exceeds the limit of 1% in a Cu alloy, it is characterized as a deliberate addition [17]. The main parts of B35 (body, lid, the lid's handle, and the rim) were made of tin bronze (Cu-Sn) alloy accompanied by a low amount of impurities (Pb, Fe, As, Ca). This type of alloy was employed in Macedonia during the Classical period for the manufacture of vessels and utensils [7,18,19]. There is a classification of bronzes from low to high Sn depending on the amount of Sn that was added to the alloy. According to the related literature, there is no single definition of the concentration of Sn that would define an ancient bronze artefact as a "high-tin" [8,12,20]. The most accepted compromise, to characterize an ancient bronze as "high-tin", is an Sn concentration between 14 wt % and 16 wt %. [21,22]. Given that the lid's handle and the rim contain enough Sn (14.42–15.62 wt %) to characterize them as "high-tin" bronzes, the body and lid are close to this definition since they contain around 12 wt % Sn. On the contrary, the hinge contains only  $6.59 \pm 0.30$  wt % Sn. The addition of Sn to Cu increases the strength and hardness of the alloy [23–25]. It also increases the resistance of the bronze artefact to corrosive parameters [21]. On the other hand, a Sn content higher than 15 wt % strongly increases the embrittlement of the alloy, raising problems (e.g., cracking) during hammering [18,25]. The role of the quantity of Sn is also significant to the appearance of bronze artefacts. A high Sn content gives them a "golden" hue which probably imitates vessels of precious metals [8,21,26] and denotes the high social status of the owner of B35; already suggested for grave goods in Derveni grave B [1]. Only the four nails are different and those contain Sn as an impurity and not as an additive [17]. Its very low level (0.06–0.76 wt %) makes the alloy easy to work with [27], but the authors also express their reservation as to whether the nails and hinge are ancient, or are modern additions. The chemical composition of bowls B43a and B43b, which are also hammered, is also different. Their main constituent is Cu (at level of 99 wt %) accompanied by a low amount of impurities (Sn, Pb, Fe, Ni, Ca). Sn is detected at very low quantities ( $0.04 \pm 0.01$  wt %) and is characterized as an impurity and not as an additive [17]. Finally, the lid of pyxis B37 presents a relatively high amount of Sn ( $12.16 \pm 0.20$  wt %), similar to the lid of case B35 ( $12.07 \pm 0.01$  wt %). The criteria of the ancient smith and their customers were more the social status and prestige imparted by the appearance of the objects [28] (ensuring the golden appearance of the artefacts with the addition of a relatively high amount of Sn) and not so much the workability. The smith of the 4th century BC probably developed skills to work with such brittle alloys without causing any cracks. The fact that pyxis B37 presents extensive corrosion compared to the good preservation of case B35 must be attributed to the taphonomic environment (e.g., the coexistence with other metal artefacts [27]) and not so with the chemical composition.

Fe is detected in all metal artefacts of the present study. In all cases, it is characterized as an impurity due to its very low concentration (0.04–0.20 wt %) [23,29]. Fe readily enters Cu during smelting and differences in Fe content arise through differences in the smelting process. The implementation of a simple and short smelting process results in an average Fe content of around 0.05 wt % instead of a process that involves slagging where the average Fe content rises at 0.5 wt % [30,31]. In this study, it is estimated that the first procedure was implemented. Moreover, for cold hammering procedures, Fe must not exceed 0.5 wt % because the formability of the artefact decreases due to precipitation phenomena [32]. Finally, the detection of very low Fe concentrations is an indicator that native and unrefined Cu was used [23,30].

Pb is considered as an impurity for all results of Table 2 since its concentration is lower than 2 wt % [33]. This is an expected result for hammered objects but not for cast ones (e.g., B35 lid's handle which contains only  $0.15 \pm 0.03$  wt % Pb). This result is unexpected since Pb was a common additive

in ancient bronzes. It improved fluidity and castability as it causes a reduction of the melting point. Most Hellenistic bronze cast artefacts contain more than 2 wt % Pb [34].

Arsenic was detected at all parts of B35 case (except the four nails) and bowls B43a and B43b at very low levels (0.01–0.04 wt %). This very small quantity may indicate that the initial ore deposit was not rich in As [33]. According to a previous study [7], Greek bronzes of the 4th century BC contain, in general, less than 1 wt % As, which is confirmed by the present investigation.

#### 4.2. Contents of the Metal Containers

Elements like Si, Al, Fe Mg, Ca, and K which were detected as the main constituents, according to the ED $\mu$ XRF analysis (Table 4), are in abundance in the earth's crust [21,27] and are consequently common soil elements. The only chemical element that is not common and is detected in all contents is Cu. A possible interpretation for this is contamination from the metal containers due to the long-term coexistence at the burial environment [35]. The other result, not common in soil, is the detection of Br in cake B35-IIa. Br was only detected in this cake, which also presents a reddish hue. The consequent implementation of the HPLC-DAD technique led to the detection of the compound 6,6'-dibromoindigotin (DBI), which is used as an index for the identification of shellfish purple (or porphyra in Greek or mollusc purple). Purple was the colour of royalty and a designator of social status.

According to the ED $\mu$ XRF results of (Table 4), the powder of pyxis B37 presents a very different chemical composition. Elements which are the main constituents in the other contents (Si, Al, Mg, Ca, K) have not been detected in B37-I. Fe and Cu oxides comprises almost 20 wt % of the powder. The rest of it could be organic material, carbon oxides, or chemical elements of a very low atomic number (lower than 12) for which the excitation conditions of the ED $\mu$ XRF technique are poor [36]. The high content of powder B37-I in ferrous constituents was also confirmed by the XRD results (Table 5), which have been normalized at 100 wt % contrary to the results of ED $\mu$ XRF (Table 4). According to them, B37-I is mostly comprised of hematite (Fe<sub>2</sub>O<sub>3</sub>), magnetite (Fe<sub>3</sub>O<sub>4</sub>), and antlerite (Cu<sub>3</sub>(SO<sub>4</sub>)(OH)<sub>4</sub>). Hematite is a red mineral pigment well known in antiquity [37]. Antlerite is a possible corrosion product of the reaction of the bronze antiquities, which are located in urban areas, with sulfur dioxide (a common pollutant). Especially in sheltered areas, the low weathering permits the accumulation of copper ions and enhancement in the acidity of water films [38].

A possible grouping according to the XRD results is: group A of the four B35 cakes where silicate minerals dominate, group B of the two B43 cakes which are mostly comprised of amorphous material, and finally group C of the red ferrous mineral powder which comprises entirely crystalline phases (Table 5). Gypsum (CaSO<sub>4</sub>·2H<sub>2</sub>O) is a common constituent in groups B and C. It is known, in antiquity, for adhesive and quick binding properties, especially regarding constructions [27]. Especially and only in the B37-I bassanite [CaSO<sub>4</sub>·0.5(H<sub>2</sub>O)], a semi-hydrous form of sulfate salt is detected. Bassanite probably resulted from the dehydration of gypsum under dried conditions. The authors, however, express their reservation that the presence of gypsum and bassanite in B37-I may be explained by contamination with reservation materials applied. In cake B35-I, the mineral hydrozincite Zn<sub>5</sub>(CO<sub>3</sub>)<sub>2</sub>(OH)<sub>6</sub>, which was used in antiquity for ophthalmic purposes, is detected [39]. The mineral cristobalite is only detected in the contents of B43a and B43b bowls. It is a member of the quartz group minerals and has the same chemical formula as quartz, SiO<sub>2</sub>, but a distinct crystal structure. The above grouping of the contents under study implies a targeted selection of raw materials in order to have the desired effects during use.

In the sample B35-IIa, pentanoic acid has been detected (Table 6). Pentanoic acid or valeric acid is a compound with an unpleasant rancid odour and naturally occurs in the roots of the plant "valeriana officinalis". It is used in pharmaceuticals, as well as in cosmetics and perfumes, in its pure form or as an ester [40]. "Valeriana officinalis" was traditionally used in ancient Greece as a treatment against stress and insomnia [41]. At the same sample, another organic substance detected is nonadecane. Nonadecane is used as a fragrance agent and it is one of the components of the essential

oils of some of the species that belong to the genus “*Artemisia*” [42]. More specifically, “*Artemisia absinthium*” is a species of *Artemisia* native to Eurasia and analysis has shown that, among several other chemical substances, its essential oil also contains nonadecane [43]. In ancient Greece, “*Artemisia absinthium*” was used for its medicinal properties against gastrointestinal disorders, as an astringent, helminthicide, diuretic, and emmenagogue [41]. In this case, nonadecane could have been used for its sole properties or as a masking agent to cover the unpleasant odour deriving from pentanoic acid. Nevertheless, access to other species of *Artemisia* or even completely different genres, not native to the Mediterranean or Eurasia, cannot be excluded. As traces of fatty acid esters can be observed in all the compartments of the lidded case (B35), a possible explanation could be a preparation in the form of an ointment or even a formulation to be consumed orally, which would target the gastrointestinal system, simultaneously combining the sedative properties of “*Valeriana officinalis*” and the therapeutic activity of *Artemisia absinthium*, as gastrointestinal disorders are commonly associated with stress.

Hexadecanoic acid was detected in the B-35-I cake. This chemical substance is also known by the name palmitic acid and is used widely as a cleansing agent and in the production of soaps [44]. Palmitic acid can be found naturally in meat, dairy products, palm oil, and palm kernel oil, as well as in other plant oils, in smaller amounts [45]. More specifically, palmitic acid is one of the constituents of the essential oil of the plant “*carum carvi*”, widely known as “caraway”, which was used in Europe as a traditional medicine for stomach disorders and flatulence [41]. The content of sample B-35-I could potentially constitute a soap or a cleansing agent, some kind of medicinal ointment, or a decoction for oral consumption to treat stomach disorders.

It is well known that fatty acids and their derivatives were used in antiquity as constituents of pharmaceutical products [41,46]. According to the results of the HS-SPME/GC-MS analysis (Table 6), many of the twenty-two organic compounds that were detected in cake B35-IIa belong to the above classes. In the same cake, 6,6'-dibromindigotin (DBI) was detected, which in combination with the reddish colour, denotes the existence of the royal dye shellfish purple. In the other cakes, very few organic compounds were detected. A possible interpretation is that cake B35-IIa was the basis that contained a large number of drastic substances and the reddish—purple colour a useful indicator for distinguishing it easily from other preparations. Alternatively, cake B35-IIa was perhaps contaminated by purple-dyed items that had been deposited in the burial. Dioscurides Pedanius, in his work “*De Materia Medica*” [46], refers to the storage of fats in tin containers for pharmaceutical purposes. The metal case B35 and pyxis B37 were made of a high tin bronze alloy, but on the other hand, bowls B43a and B43b were made of almost pure Cu.

## 5. Conclusions

The combination of spectrometric (ED $\mu$ XRF, XRD) and chromatographic (HPLC-DAD, HS SPME/GC-MS) analytical techniques was used as a holistic archaeometric approach in order to determine the construction technology of a group of metal containers and the chemical synthesis of their contents. The analytical methodology gave priority to a non-destructive implementation, as far as possible, due to the uniqueness and significance of the analyzed material. For the elemental analysis of the metal containers, ED $\mu$ XRF spectrometry was implemented, in a non-invasive way, which resulted in the determination of their raw materials. Moreover, differentiations in their constituent parts were found. Generally, two kinds of alloy were used: a high tin bronze alloy for the construction of the main parts of metal case B35 and pyxis B37 and pure Cu accompanied by a low amount of impurities for the manufacture of bowls B43a and B43b. Furthermore, their chemical composition reveals the ancient archaeometallurgical procedures of the 4th century BC.

The implementation of a non-invasive technique like ED $\mu$ XRF could be used as a guide for the selective implementation of a destructive one, e.g., the detection of Br in cake B35-IIa, which led to the implementation of HPLC-DAD and the detection of the royal dye shellfish purple. Although the archaeological approach led to the conclusion that this set was used for medical purposes [4],

the archaeometric approach provides us with further information on medical knowledge in Macedonia during the 4th century BC

**Author Contributions:** Conceptualization, C.S.K., D.I.; Methodology, C.S.K., D.I., G.A.Z.; Investigation, C.S.K., A.Z., N.K., I.K.; Writing-Original Draft Preparation, C.S.K., D.I., N.K., I.K.; Writing-Review & Editing, C.S.K.; G.A.Z.; Supervision, G.A.Z.

**Funding:** This research received no external funding.

**Acknowledgments:** The authors wish to thank: P. Adam—Veleni, then Director of the Archaeological Museum of Thessaloniki (A.M.Th.) for the permission to analyze the artefacts of the article; V. Michalopoulou, Conservator of Antiquities, A.M.Th., for providing support with issues concerning ancient technology and metal conservation; and the two anonymous reviewers for their recommendations which resulted in a greatly improved paper.

**Conflicts of Interest:** The authors declare no conflict of interest.

## References

- Themelis, P.; Touratsoglou, G. *The tombs of Derveni*; Ministry of Culture—Archaeological Receipts Fund: Athens, Greece, 1977. (In Greek) (Θέμελης, Π., Τουράτσογλου, Γ., 1997. Ο ι τάφοι του Δερβενίου, Υπουργείο Πολιτισμού—Ταμείο Αρχαιολογικών Πόρων και Απαλλοτριώσεων, Αθήνα)
- Tsigarida, B.; Ignatiadou, D. *The Gold of Macedonia: Archaeological Museum of Thessaloniki, Archaeological Receipts Fund*; Archaeological Museum of Thessaloniki: Thessaloniki, Greece, 2000.
- Chrysostomou, P. Contributions to the history of medicine in ancient Macedonia. *Eulimene* **2002**, *3*, 99–116. (In Greek) (Χρυσοστόμου, Π. 2002, «Συμβολές στην Ιστορία της Ιατρικής στην Αρχαία Μακεδονία», Ευλιμένη *3*, 99–116»)
- Ignatiadou, D. The warrior priest in Derveni grave B was a healer too, *Histoire. Méd. Santé* **2016**, *8*, 89–113. [[CrossRef](#)]
- Guerra, M.F. Analysis of archaeological metals, The place of XRF & PIXE in the determination of technology and provenance. *X-ray Spectrom.* **1998**, *27*, 73–80.
- Cechak, T.; Hlozek, M.; Musilek, L.; Trojek, T. X-ray fluorescence in investigations of archaeological finds. *Nucl. Instrum. Methods Phys. Res. Sect. B* **2007**, *B263*, 54–57. [[CrossRef](#)]
- Karydas, A.G. Application of a portable XRF spectrometer for the non invasive analysis of museum metal artefacts. *Ann. Chim.* **2007**, *97*, 419–432. [[CrossRef](#)] [[PubMed](#)]
- Charalambous, A.; Kassianidou, V.; Papisavvas, G. A compositional study of Cypriot bronzes dating to the Early Iron Age using portable X-ray fluorescence spectrometry (pXRF). *J. Archaeol. Sci.* **2014**, *46*, 205–216. [[CrossRef](#)]
- Stuart, B. *Analytical Techniques in Materials Conservation*; John Wiley & Sons Ltd.: Chichester, UK, 2007; p. 194.
- Bronk, H.; Rohrs, S.; Bjeoumikhov, A.; Langhoff, N.; Schmalz, J.; Wedell, R.; Gorny, H.-E.; Herold, A.; Waldschlager, U. Artax—A new mobile spectrometer for EDXRF spectrometry on art & archaeological objects, Fresenius' *J. Anal. Chem.* **2001**, *371*, 307–316.
- Dylan, S. Handheld XRF analysis of Renaissance bronzes: Practical approaches to quantification and acquisition. In *Handheld XRF for Art and Archaeology*; Shugar, A.N., Mass, J.L., Eds.; Leuven University Press: Leuven, The Netherlands, 2012; pp. 37–74.
- Scott, D.A. *Ancient Metals: Microstructure and Metallurgy*; Lulu.com: Morrisville, NC, USA, 2010; Volume I.
- Klug, H.P.; Alexander, L.E. *X-ray Diffraction Procedures for Polycrystalline and Amorphous Materials*; John Wiley & Sons: New York, NY, USA; Sydney, Australia; Toronto, ON, Canada, 1974; 966p.
- Kantiranis, N.; Stergiou, A.; Filippidis, A.; Drakoulis, A. Calculation of the percentage of amorphous material using PXRD patterns. *Bull. Geol. Soc. Greece* **2004**, *36*, 446–453.
- Vasileiadou, A.; Karapanagiotis, I.; Zotou, A. Determination of Tyrian purple by high performance liquid chromatography with diode array detection. *J. Chromatogr. A* **2016**, *1448*, 67–72. [[CrossRef](#)] [[PubMed](#)]
- Karapanagiotis, I.; Mantzouris, D.; Cooksey, C.; Mubarak, M.S.; Tsiamyrtzis, P. An improved HPLC method coupled to PCA for the identification of Tyrian Purple in archaeological and historical samples. *Microchem. J.* **2013**, *110*, 70–80. [[CrossRef](#)]
- Healy, J.F. *Mining and Metallurgy in the Greek and Roman World*; Thames and Hudson: London, UK, 1978.

18. Varoufakis, G. Technological specifications of the 4th century BC. Contribution to the historic metallurgy. *Archaeol. Ephemer.* **1974**, *113*, 57–62. (In Greek). (Βαρουφάκης, Γ., 1974. Τεχνικά προδιαγραφαί του 4<sup>ου</sup> αι. π.Χ. Συμβολή εις την ιστορικήν μεταλλουργίαν, Αρχαιολογική Εφημερίς, σελ. 57–62)
19. Asiminos, K. Macedonian metalworking and alloy composition of the classical era. In Proceedings of the XII International Congress of Classical Archaeology, Athens, Greece, 4–10 September 1983; Volume C, pp. 283–288. (In Greek) (Ασημενός, Κ., 1988. Μακεδονική μεταλλοτεχνία και σύσταση κραμάτων της κλασικής εποχής, στο XII Διεθνές Συνέδριο Κλασικής Αρχαιολογίας, τόμος Γ', Αθήνα, σελ. 283–288)
20. Scott, D.A. *Metallography and Microstructure of Ancient and Historic Metals*; The Getty Conservation Institute: Singapore, 1991.
21. Ashkenazi, D.; Iddan, N.; Tal, O. Archaeometallurgical characterization of Hellenistic metal objects: The contribution of the objects for Rishon Le-Zion (Israel). *Archaeometry* **2012**, *54*, 528–548. [[CrossRef](#)]
22. Konečná, R.; Fintová, S. Copper and copper alloys: Casting, classification and characteristic microstructures. In *Copper Alloys—Early Applications and Current Performance—Enhancing Processes*; Collini, L., Ed.; InTech Web.Org: Rijeka, Croatia, 2012; pp. 3–30.
23. Tylecote, R.F. *The Early History of Metallurgy in Europe*; Longman Inc.: New York, NY, USA, 1987.
24. Craddock, P.T. The composition of the copper alloys used by the Greek, Etruscan and Roman civilisations: 2. the Archaic, Classical and Hellenistic Greeks. *J. Archaeol. Sci.* **1977**, *4*, 103–123. [[CrossRef](#)]
25. Craddock, P.T. The composition of the copper alloys used by the Greek, Etruscan and Roman Civilizations. *J. Archaeol. Sci.* **1976**, *3*, 93–113. [[CrossRef](#)]
26. Figueiredo, E.; Silva, R.J.C.; Senna-Martinez, J.C.; Araújo, M.F.; Braz Fernandes, F.M.; Inês Vaz, J. Smelting and recycling evidences from the Late Bronze Age habitat site of Baiões (Viseu, Portugal). *J. Archaeol. Sci.* **2010**, *37*, 1623–1634. [[CrossRef](#)]
27. Goffer, Z. *Archaeological Chemistry*, 2nd ed.; John Wiley & Sons, Inc.: Hoboken, NJ, USA, 2007.
28. Descamps- Lequime, S. The color of bronze—Polychromy and the aesthetics of bronze surfaces. In *Power and Pathos—Bronze Sculpture of the Hellenistic World*; Daehner, J.M., Lapatin, K., Eds.; J. Paul Getty Museum: Los Angeles, CA, USA, 2015; pp. 150–165.
29. Craddock, P.T.; Meeks, N.D. Iron in ancient copper. *Archaeometry* **1987**, *29*, 187–204. [[CrossRef](#)]
30. Henderson, J. *The Science and Archaeology of Materials—An Investigation of Inorganic Materials*; Routledge: New York, NY, USA, 2000.
31. Cooke, S.R.B.; Aschenbener, S. The occurrence of metallic iron in ancient copper. *J. Field Archaeol.* **1975**, *2*, 251–266.
32. Papadimitriou, G. Copper and bronze metallurgy in ancient Greece. In *Archaeometry 90, Proceedings of the International Symposium in Archaeometry, 2–6 April 1990, Heidelberg, Germany*; Wagner, G.A., Pernicka, E., Eds.; Birkhauser Verlag: Basel, Switzerland, 1991; pp. 117–126.
33. Oudbashi, O.; Davami, P. Metallography and microstructure interpretation of some archaeological tin bronze vessels from Iran. *Mater. Charact.* **2014**, *97*, 74–82. [[CrossRef](#)]
34. Craddock, P.T.; Giunlia-Mair, A. Problems and possibilities for provenancing bronzes by chemical composition. In *Bronzeworking Centers of Western Asia, c.100-539 B.C., Kegan Paul International in Association with the British Museum*; Curtis, J., Ed.; Kegan Paul International in association with the British Museum; Distributed by Routledge; Chapman & Hall: London, UK, 1988.
35. Rovira, S.; Montero, I. Natural tin-bronze alloy in Iberian Peninsula metallurgy: Potentiality and reality. In *The Problem of Early Tin*; Giunlia-Mair, A., Schiavo, F.L., Eds.; Archaeopress: Oxford, UK, 2003; pp. 15–22.
36. Jenkins, R. *X-ray Fluorescence Spectrometry*; John Wiley & Sons Inc.: Hoboken, NJ, USA, 1999.
37. Gettens, R.J.; Stout, G.L. *Paintings Materials: A Short Encyclopedia*; Dover Publications: New York, NY, USA, 1966.
38. Leygraf, C.; Graedel, T.E. *Atmospheric Corrosion*; Wiley-Interscience: New York, NY, USA, 2000.
39. Giachi, G.; Pallecchi, P.; Romualdi, A.; Ribechini, E.; Lucejko, J.J.; Colombini, M.P.; Lippi, M.M. Ingredients of a 2000-y-old medicine revealed by chemical, mineralogical and botanical investigations. *PNAS* **2013**, *110*, 1193–1196. [[CrossRef](#)] [[PubMed](#)]
40. Goldberg, I.; Rokem, J.S. Organic and Fatty Acid Production, Microbial. In *Encyclopedia of Microbiology*, 3rd ed.; Elsevier: New York, NY, USA, 2009; pp. 421–442.

41. Skaltsa, E. *History of Pharmacy*; Kallipos-Hellenic Academic Books: Athens, Greece, 2015; p. 104. (In Greek) (Σκαλτσά, Ε., 2015. «Ιστορία της Φαρμακευτικής», Κάλλιπος-Ελληνικά Ακαδημαϊκά Συγγράμματα και Βοηθήματα, Αθήνα, 104)
42. Mojarrab, M.; Delazar, A.; Esnaashari, S.; Afshar, F.H. Chemical composition and general toxicity of essential oils extracted from the aerial parts of *Artemisia armeniaca* Lam. and *A. incana* (L.) Druce growing in Iran. *Res. Pharm. Sci.* **2013**, *1*, 65–69.
43. Kordali, S.; Cakir, A.; Mavi, A.; Kilic, H.; Yildirim, A. Screening of Chemical Composition and Antifungal and Antioxidant Activities of the Essential Oils from Three Turkish *Artemisia* Species. *Agric. Food Chem.* **2005**, *53*, 1408–1416. [[CrossRef](#)] [[PubMed](#)]
44. Anneken, D.J.; Both, S.; Christoph, R.; Fieg, G.; Steinberner, U.; Westfechtel, A. Fatty Acids. In *Ullmann's Encyclopedia of Industrial Chemistry*; Wiley-VCH: Weinheim, Germany, 2006.
45. Kim, S.; Thiessen, P.A.; Bolton, E.E.; Chen, J.; Fu, G.; Gindulyte, A.; Han, L.; He, J.; He, S.; Shoemaker, B.A.; et al. PubChem Substance and Compound databases. *Nucleic Acids Res.* **2016**, *44*, D1202–D1213. [[CrossRef](#)] [[PubMed](#)]
46. Dioscorides, P. *De Materia Medica*; Beck, L.Y., Translator; *Altertumswissenschaftliche Texte und Studien*, Band 38; Olms-Weidmann: Hildesheim, Germany, 2005.



© 2018 by the authors. Licensee MDPI, Basel, Switzerland. This article is an open access article distributed under the terms and conditions of the Creative Commons Attribution (CC BY) license (<http://creativecommons.org/licenses/by/4.0/>).